Deep-Sea Research II 120 (2015) 91–102

Contents lists available at ScienceDirect

Deep-Sea Research II

journal homepage: www.elsevier.com/locate/dsr2

Microzooplankton community structure and grazing impact on major phytoplankton in the Chukchi sea and the western Canada basin, Arctic ocean

Eun Jin Yang [a,*], Ho Kyung Ha [b], Sung-Ho Kang [a]

[a] Division of Polar Ocean Environment, Korea Polar Research Institute, 213-3 Songdo-dong, Yeonsu-gu, Incheon 406-840, Republic of Korea
[b] Department of Ocean Sciences, Inha University, Incheon 402-751, Republic of Korea

ARTICLE INFO

Available online 10 July 2014

Keywords:
Microzooplankton
Grazing rate
Growth rate
Chukchi Sea
Canada Basin

ABSTRACT

We investigated the microzooplankton community and its grazing impact on major phytoplankton groups in the Chukchi Sea and in the western Canada Basin during the period July–August 2010. The study area was divided into three regions based on topography, hydrographic properties and trophic conditions: (1) a productive region over the Chukchi Sea shelf (CSS) with high phytoplankton biomass dominated by diatoms, (2) an oligotrophic region over the Northwind Abyssal Plain (NwAP) with low phytoplankton biomass dominated by picophytoplankton, and (3) the Northwind Ridge (NwR), over which waters were dominated by picophytoplankton and diatoms. The spatial distribution of microzooplankton biomass and its composition were related to differences in phytoplankton biomass and assemblage composition in the three water masses. Heterotrophic dinoflagellates (HDF) and ciliates were significant components of microzooplankton populations. Athecate HDF was the most important component in the CSS, where diatoms were dominant. Naked ciliates were dominant microzooplankton in the NwR. Microzooplankton grazing rate varied by the assemblage composition of both phytoplankton and microzooplankton. Microzooplankton was capable of consuming an average of 71.7 ± 17.2% of daily phytoplankton production. Growth rates of smaller phytoplankton (i.e., picophytoplankton and autotrophic nanoflagellates) and grazing rates on them were higher than rates for diatoms. Microzooplankton grazed more on picophytoplankton (PP grazed = 89.3 ± 20.5%) and autotrophic nanoflagellates (PP grazed = 82.3 ± 22.5%) than on diatoms (PP grazed = 62.5 ± 20.5%). The dynamics of predator and prey populations were almost balanced in waters in which smaller phytoplanktons were dominant. Picophytoplankton production was consumed by microzooplankton allowing transfer to larger consumers. On average, microzooplankton grazed 62.5% of the diatom production in the waters we studied, indicating that the classical food chain (with carbon flux from diatoms to copepods) is likely operational and of significance in this region. Overall, microzooplankton grazing was an important process controlling phytoplankton biomass and composition in the Chukchi Sea and the western Canada Basin during early summer.

1. Introduction

Microzooplankton are key components of pelagic food webs. They are important grazers of phytoplankton and act as a food source for consumers at higher trophic levels. These micro-grazers are highly abundant, ubiquitous in the world's oceans, grow rapidly and have unique feeding mechanisms that allow ingestion of wide spectrum of food particle sizes. This combination of attributes makes micrograzers essential elements in the functioning of pelagic ecosystems (Hansen et al., 1994; Sherr and Sherr, 2002; Calbet and Landry, 2004; Calbet and Saiz, 2005; Saiz and Calbet, 2011). Microzooplankton community structure and grazing pressure are drivers of top-down control pressure on phytoplankton in pelagic ecosystems. These drivers may restructure phytoplankton assemblages when grazing is selective, and they influence the functioning of the microbial food web (Burkill et al., 1987; Reckermann and Veldhuis, 1997; Irigoien et al., 2005; Calbet, 2008; Yang et al., 2012). Consequently, the details of microzooplankton community structure and the net grazing impact on phytoplankton are crucial for an expanded understanding of carbon flow and the fate of primary production in marine ecosystems.

In the western Arctic Ocean, the broad and shallow Chukchi shelf links the Pacific and the Arctic Oceans. During transit through

* Corresponding author. Tel.: +82 32 760 5334; fax: +82 32 760 5399.
E-mail address: ejyang@kopri.re.kr (E.J. Yang).

http://dx.doi.org/10.1016/j.dsr2.2014.05.020
0967-0645/

the Chukchi Sea, Pacific waters flowing from the Bering Strait are significantly modified by oceanic and atmospheric forcings. These mechanisms play a significant role in the stratification and circulation of the western Arctic Ocean (Aagaard et al., 1981). A combination of seasonally variable environmental factors and the inflow of warm Pacific water result in spatial and temporal variability of the water mass in the western Arctic Ocean (Carmack and Wassmann, 2006). Thus, productivity and plankton composition in this region are regulated by physical forcing and hydrographic characteristics of the water mass (Ashjian et al., 2003; Grebmeier and Harvey, 2005; Lane et al., 2008; Sukhanova et al., 2009). The Arctic Ocean is currently undergoing rapid environmental change resulting from natural and anthropogenic drivers, which include accelerated warming (Steele et al., 2008; Zhang et al., 2010), decreased extent of sea ice cover (e.g., Comiso et al., 2008) and other physical changes. These changes will have a major impact on ecosystem functioning and biogeochemical cycling in the Arctic Ocean (e.g., Sakshaug and Slagstad, 1992; Walsh et al., 2004). Because of ongoing changes in the Arctic, there is an urgent imperative for better characterization and understanding of food web structures that are key elements of the Arctic pelagic ecosystem.

Comprehensive studies of pelagic Arctic microzooplankton assemblages have generally been limited to the central Arctic Ocean, including the Chukchi Sea (Sherr et al., 1997; Sherr et al., 2003; Sherr et al., 2009), the Bering Sea (Olson and Strom, 2002; Strom and Fredrickson, 2008; Sherr et al., 2013), western Greenland (Nielsen and Hansen, 1995; Levinsen et al., 1999, 2000; Levinsen and Nielsen, 2002), and the Barents Sea (Verity et al., 2002). Previous studies have emphasized the importance of microzooplankton in microbial assemblages and their role as major consumers of phytoplankton. Campbell et al. (2009) reported that microzooplankton were generally preferred over phytoplankton as prey for copepods in the western Arctic Ocean. However, other studies have described low levels of microzooplankton grazing on phytoplankton during the spring and summer seasons in portions of the high Arctic Ocean (Sherr et al., 2009; Calbet et al., 2011). Most Arctic studies of microzooplankton have been conducted in eastern Arctic waters, coastal, bays and/or relatively low latitude sites. At the present time, the high-latitude marine ecosystem is particularly sensitive to climate change because small temperature differences can have large effects on the extent and thickness of sea ice (Holland et al., 2006). However, the role of microzooplankton in food webs of the high-latitude sectors of Arctic Ocean remains uncertain. The work reported here is a first step toward improved understanding of the role of microzooplankton in high-latitude waters of the western Arctic Ocean (73–78°N).

The results of this study emphasize the need for further research for a broader perspective on the phytoplankton–microzooplankton trophic link in pelagic ecosystems of high-latitude Arctic Ocean. We investigated spatial variation of microzooplankton assemblages and their grazing impacts on phytoplankton in different waters during early summer to determine the relative importance of microzooplankton composition in different geographic regions through its effect on the grazing pressure exerted on major phytoplankton groups.

2. Materials and methods

The Korea Arctic Research Program mounted a multidisciplinary expedition in the Pacific sector of the Arctic Ocean aboard the *IBRV* Araon icebreaker during the period 17 July–14 August 2010. The study area included (1) the Chukchi Sea shelf (CSS; stns 1, 38, 3, 4, 35), (2) the Northwind Abyssal Plain (NwAP; stns 33, 32, 31, 28, 29), and (3) the Northwind Ridge (NwR; stns 6, 8, 10, 13, 14) (Fig. 1).

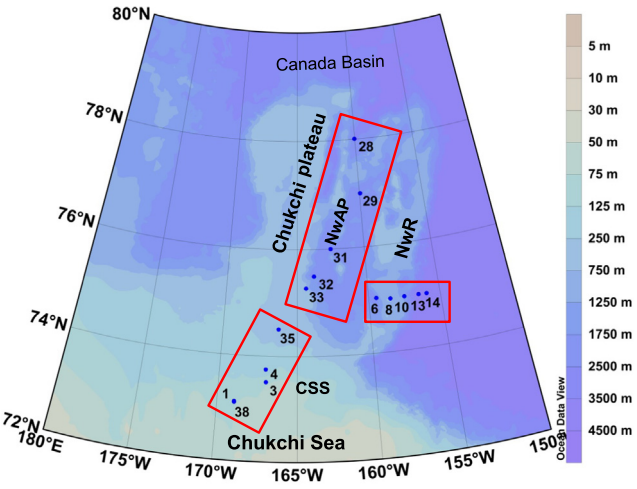

Fig. 1. Sampling stations in the western Arctic Ocean from 17 July to 14 August, 2010. NwAP, Northwind Abyssal Plain; NwR, Northwind Ridge; and CSS, Chukchi Sea shelf.

2.1. Collection and analysis of hydrographic data

At all the stations, we made hydrocasts to make measurements of conductivity/temperature/depth (CTD) (SeaBird Electronics, SBE 911plus) that were used to plot vertical profiles of temperature and salinity. Using traditional *T–S* (temperature–salinity) diagram analyses, we determined the mixing and transformation of water masses. To collect water samples for measurements of chlorophyll-*a* (Chl-*a*) concentration, we installed 12 Niskin bottles (20 l each) on the CTD frame to sample waters at depths of 3, 10, 20, 30, 75, 100 m and at the depth of the subsurface chlorophyll maximum (SCM). Water subsamples (1 l) were filtered through glass-fiber filter paper (25 mm; Gelman); Chl-*a* concentrations were measured with a Turner Designs fluorometer (TD-700) following extraction in 90% acetone (Parson et al., 1984). The fluorometer had been previously calibrated against pure Chl-*a* (Sigma-Aldrich).

2.2. Phytoplankton and microzooplankton

To determine abundances of microzooplankton by depth, we used a Niskin rosette sampler to collect water samples at 3, 10, 20, 30, SCM, 75, and 100 m depths. Water samples for phytoplankton biomass analysis were taken from 10 m and at the SCM depth, the two depths for which dilution experiments were conducted at each station. To determine the abundance of plankton other than ciliates and diatoms, we preserved 500 ml samples of water with glutaraldehyde (1% final concentration), then stored them at 4 °C before staining and filtration. Subsample of 100 ml was filtered onto nuclepore filters (0.8 μm pore size, black) for 3–20 μm sized plankton and 300 ml subsample was filtered onto nuclepore filters (8 μm pore size, black) for >20 μm sized plankton. For picophytoplankton (<3 μm sized), subsample of 20–40 ml was filtered onto nuclepore filters (0.2 μm pore size, black). Aliquots of the preserved samples were stained with proflavin (0.33%) for an hour before filtration. During filtration, the samples were drawn down until 5 ml remained in the filtration tower. Concentrated DAPI (50 μg ml^{-1} final concentration) was then added and allowed to sit briefly (5 s) before filtering the remaining sample until dry (Taylor et al., 2011). Filters were mounted onto glass slides with immersion oil and cover slips. For nano-and microplankton cells, at least 50 fields per sample were counted with an epifluorescence

microscope (Olympus BX 51) at magnifications of 200–640 × using blue light excitation filter set for chlorophyll autofluorescence and UV light excitation filter set for DAPI stained cells. Autotrophic organisms were distinguished from heterotrophs by the presence of chlorophyll, which was visualized as red fluorescence under blue light illumination. For picophytoplankton cells, at least 200 cells per sample were counted with an epifluorescence microscope (Olympus BX 51) at magnifications of 1000 × using blue light excitation. Picoeukaryotes and picocyanobacteria were identified by their red and orange autofluorescence as observed under the blue light illumination. During inspection of picophytoplankton samples, picocyanobacteria were rarely observed from all samples.

For ciliates and diatoms, 500 ml samples of water were preserved with 4% acid Lugol's iodine solution and subsequently stored in darkness. Preserved samples were allowed to settle in the mass cylinder for at least 48 h. The upper water layer was then siphoned out, leaving 50 ml. Subsequently, 5–20 ml from each sample were settled in sedimentation chambers before enumeration under an inverted compound microscope (Olympus IX 70). Samples were counted within 3 months of sampling dates. To estimate the carbon biomass of plankton, cells were sized using image analysis system standardized by a calibrated ocular micrometer and calculated cell volume by measuring cell dimensions (Edler, 1979). Microzooplankton were classified as heterotrophic nanoflagellates (HNF), choanoflagellates (CNF), ciliates, heterotrophic dinoflagellates (HDF) and radiolarians. Phytoplankton were classified as picophytoplankton, autotrophic nanoflagellates (ANF), autotrophic dinoflagellates (ADF) and diatoms. The following conversion factors and equations were used to transform cell volumes into carbon biomass: 0.19 μg C μm^{-3} for naked ciliates (Putt and Stoecker, 1989); carbon (pg)=445.0+0.053 lorica volume (μm^3) for loricate ciliates (Verity and Langdon, 1984); carbon (pg)=0.216 × [volume, μm^3]$^{0.939}$ for dinoflagellates and diatoms (Menden-Deuer and Lessard, 2000); and 220 fg C μm^{-3} for nanoflagellates and picophytoplankton (Bøsheim and Bratbak, 1987). For radiolarians, we used the equation of Michaels et al. (1995)

2.3. Grazing experiments

We estimated phytoplankton growth and microzooplankton grazing rates by the dilution method through measurements of changes in total Chl-*a* concentration and major phytoplankton biomass over time (Landry and Hassett, 1982). All equipments for the grazing experiments were cleaned with 10% HCl in Milli-Q water and rinsed thoroughly thrice in Milli-Q water before experiments. Plastic gloves were worn during all phases of the experiments. Water for grazing experiments was collected from within the surface mixed layer at 10 m depth and in the SCM layer. At each station, 40 l seawater were collected in a Niskin bottle and transferred to a polycarbonate carboy. Water was prepared by gravity filtration from the water bottle through an in-line filter capsule (Gelman Critcap 100, 0.2 μm pore size filter, pre-washed with 10% trace-metal grade HCl followed by Milli-Q and seawater rinses) into a clean polycarbonate bottle. The prepared water was then diluted with 0.2 μm filtered seawater to obtain duplicates containing the following proportions of prepared water: 100%, 75%, 55%, 30%, and 11%. The dilution series was established in ten 2l polycarbonate bottles to each of which we added a nutrient mixture (5 μM NH_4Cl, and 1 μM Na_2HPO_4) to ensure that minerals did not become limiting during incubation. Two additional undiluted experimental bottles (i.e., 100% strength prepared water bottles) were made up without nutrients to serve as no-nutrient supplementation controls. All dispensing was conducted gently to avoid cell rupture and damage. The bottles were incubated on deck for 48 h at ambient sea surface temperatures and screened to ambient light levels with neutral density screens. Subsamples were collected for each experiment at the beginning (T_0, undiluted treatment bottle) and at the end (T_{48}, each treatment bottle) of the incubation to estimate Chl-*a* concentrations and phytoplankton biomass for each groups as described above. The prey was classified into phytoplankton four groups (picophytoplankton, ANF, ADF and Diatom) and total Chl-*a* concentration.

We used a linear regression model for all experiments to find the best-fit relationship between phytoplankton net growth rate and dilution level (Landry and Hassett, 1982). Phytoplankton growth with nutrient enrichment (μ_n) and grazing rate (g) were estimated from the y-intercept and the negative slope of the relationship, respectively. Because the intercept of the equation overestimated phytoplankton growth rates (nutrients had been added to the bottles), instantaneous phytoplankton growth rates (μ) were derived from the net phytoplankton growth rate (μ_o) in the undiluted bottles without added nutrients plus the grazing rate (g) of microzooplankton in the dilution experiments ($\mu=\mu_o+g$). The impacts of microzooplankton grazing on phytoplankton production (%PP) and phytoplankton standing stock (%PS) were determined following the calculation procedures of Verity et al. (1993). All statistical tests were performed using the SPSS software (ver. 9.0).

3. Results

3.1. Hydrographic features

Fig. 2 plots the spatial distribution of temperature and salinity. The water column appeared to be stratified with a strong pycnocline between (i) the surface mixed layer with low temperature and salinity and (ii) Pacific Summer Water (PSW) with high temperature and salinity. In the vicinity of CSS (stns 38 and 4), relatively dense water below 30 m depth was distributed across the continental slope. On the other hand, the warm water pool, as mesoscale warm-core eddy, occurred at the depth of 50–80 m between stns 32 and 28 in the NwAP. Interestingly, a subsurface warm-core eddy was clearly recognizable in the cross-transect of the NwR. The eddy was ca. 25 km in diameter and had a maximum temperature of about 0.5 °C. The isohaline and isothermal plots tracked concave-up trajectories indicative of warm-core eddies. Through water mass identification, we demonstrated that core water at depths of 30–130 m originated from PSW, while the underlying water mass comprised Pacific Winter Water (PWW). PSW was a relatively warm, fresh water mass with salinities in the range of 30–32 and temperatures of −1.5 to 0.2°C. PWW was a layer of relatively fresh (i.e., buoyant), cold water lying immediately below the PSW. The small scale features, such as Pacific water eddies that we observed at stn 13, had domed isohalines with warm caps above them.

3.2. Chlorophyll-a concentrations, phytoplankton biomass and composition

Chl-*a* concentrations varied widely among stations and depths during the study period (Fig. 3). Distinct SCM layers appeared at depths of 40–60 m. Concentration varied in the range of 0.01–3.65 μg l^{-1}, with an average of 0.34 ± 0.71 μg l^{-1} (mean ± SD). There was an extremely high Chl-*a* concentration (> 3 μg l^{-1}) in the SCM layer at stns 4 and 13. Depth-averaged Chl-*a* in the CSS was higher than concentrations in the NwAP and NwR.

The phytoplankton assemblages varied considerably in both composition and biomass (Fig. 4). There were obvious differences between the surface and SCM layers. Diatoms and picophytoplankton

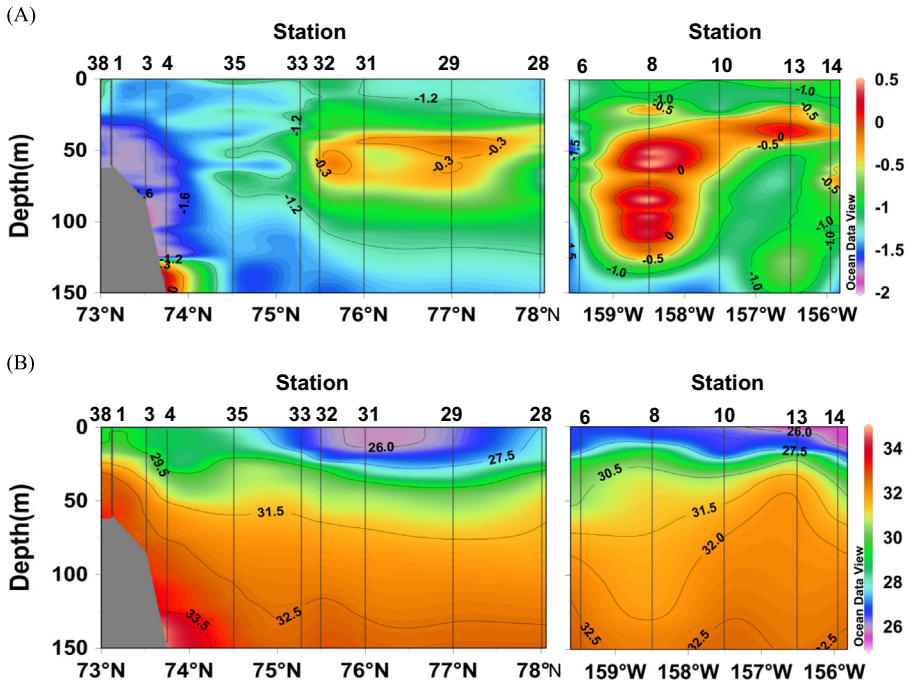

Fig. 2. Vertical section of temperature (A) and salinity (B) in the western Arctic Ocean.

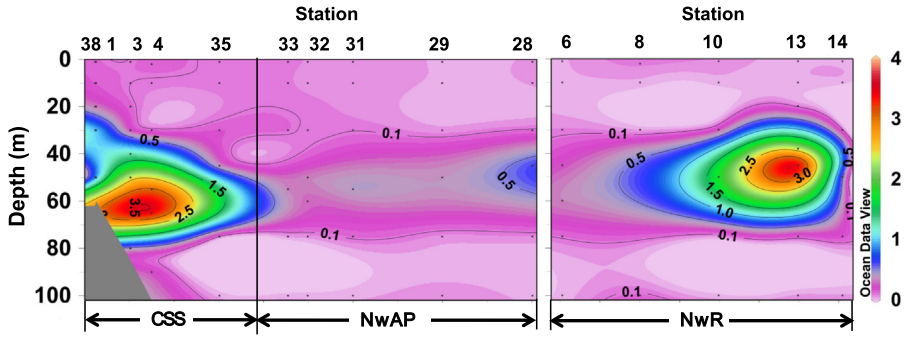

Fig. 3. Vertical section of chlorophyll-*a* concentration ($\mu g\, l^{-1}$) in the western Arctic Ocean. NwAP, Northwind Abyssal Plain; NwR, Northwind Ridge; and CSS, Chukchi Sea shelf.

were predominant. Diatoms were an important fraction of phytoplankton biomass in the CSS and in the SCM layer of the NwR. Pelagic diatom species; e.g., *Chaetocerous* spp. and *Thalassiosira* spp., dominated the phytoplankton when Chl-*a* concentrations were in the range 2.0–3.5 $\mu g\, l^{-1}$. At the lower Chl-*a* concentration in the NwAP and in the surface layer of the NwR, there was a mixed species assemblage of picophytoplankton, ANF, ADF and smaller chained diatoms. Picophytoplankton accounted for $>50\%$ of phytoplankton biomass in the NwAP and in the surface layer of the NwR.

3.3. Microzooplankton abundance, biomass and community composition

The abundances of microzooplankton components varied among oceans sectors and depths (Fig. 5). The abundance of HNF, including CNF, ranged from 73 to 2700 cells ml^{-1}, averaging 520 ± 517 cells ml^{-1}. High HNF abundances occurred in the SCM layer at the CSS. The ciliate assemblages were numerically dominated by naked ciliates. Although a few loricate ciliates occurred in the CSS and NwAP, they represented only a small fraction of the total ciliate abundance. The abundances of ciliates ranged from 17 to 5620 cells l^{-1}, averaging 763 ± 840 cells l^{-1}. Ciliates were most abundant in the CSS and NwAP, and extremely abundant in the SCM layer at stn 8. A small fraction of ciliate abundance comprised chloroplast-bearing species, especially in the NwR. Mixotrophic ciliates, such as *Laboea strobila*, and *Strombidium conicum*, contributed 20–30% to total ciliate abundance in the NwR, particularly in stns 8 and 13 (data not shown). HDF were numerically dominated by athecate HDF, which were further categorized into nanoHDF ($<20\,\mu m$) and microHDF ($>20\,\mu m$), the abundances of which ranged from 1000 to 190,000 cells l^{-1} (average, $24{,}500 \pm 24{,}200$ cells l^{-1}) and from 74 to 3770 cells l^{-1} (average, 532 ± 725 cells l^{-1}), respectively. The abundances of microHDF were highest in the CSS and in the SCM layer of the NwR; nanoHDF were relatively abundant in the CSS and in the SCM layer of stn 6.

Microzooplankton biomass ranged from 0.6 to 42.9 $\mu g\, C\, l^{-1}$ (average, $9.1 \pm 8.7\ \mu g\, C\, l^{-1}$) and was relatively high in SCM layers at all stations (Fig. 6). Depth-integrated microzooplankton biomass from the surface to 100 m ranged from 358.4 to 1666.9 mg C m^{-2}, averaging 727.9 mg C m^{-2}. Highest microzooplankton biomass occurred in the CSS; the lowest biomass occurred in the NwAP (Fig. 6). Ciliates and HDF comprised the largest proportion of the microzooplankton assemblage. Depth-integrated ciliate biomass

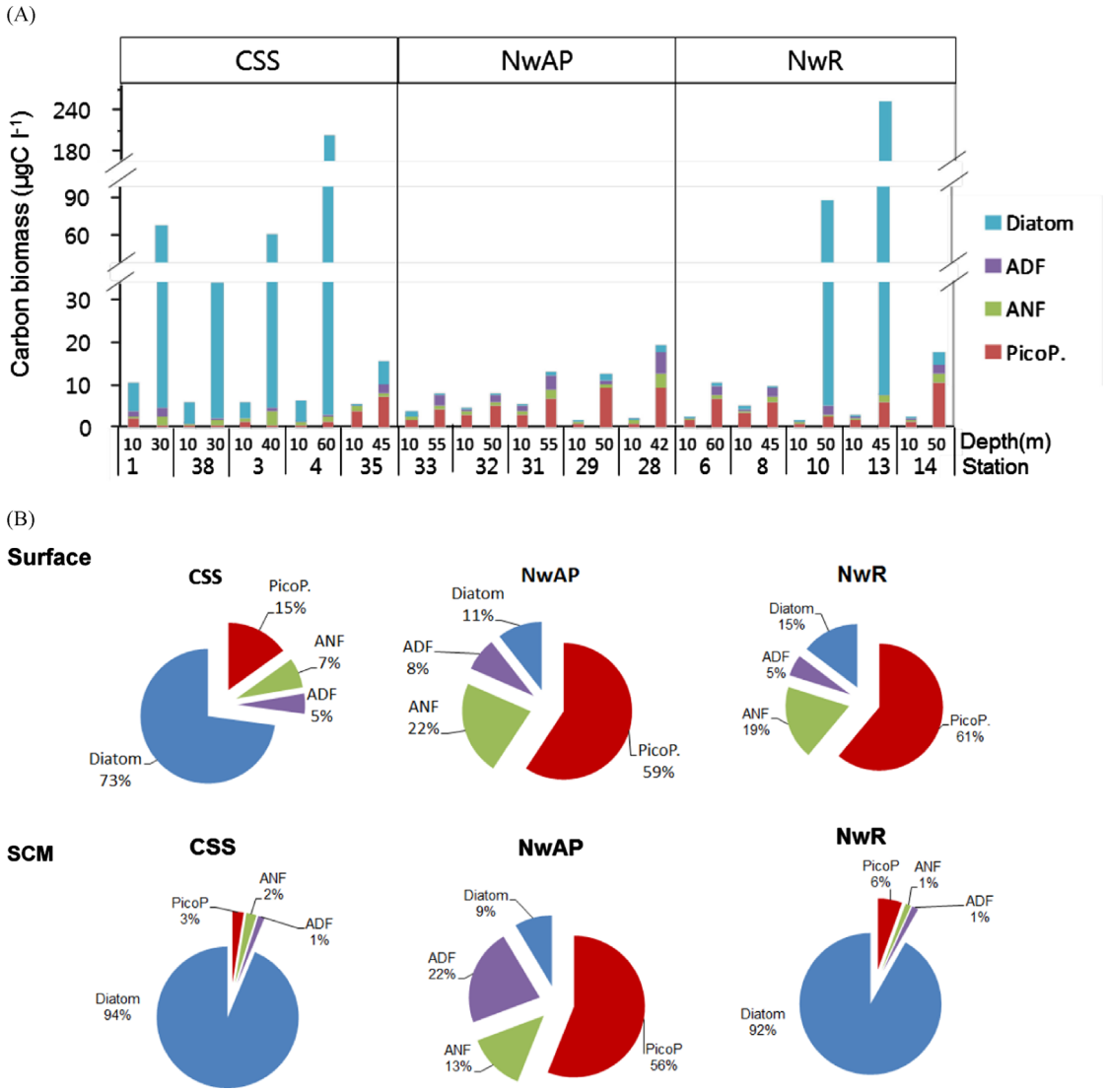

Fig. 4. Distribution of phytoplankton biomass (A) and community structure (B) in the western Arctic Ocean. ANF, autotrophic nanoflagellate; ADF, autotrophic dinoflagellate; and PicoP, picophytoplankton.

ranged from 184.2 mg C m^{-2} in the NwR to 312.8 mg C m^{-2} in the CSS. On average, 45% of total biomass in the NwR comprised ciliates, but they contributed a smaller proportion (average, 26%) to the total in the CSS. Depth-integrated HDF biomass ranged from 723.2 mg C m^{-2} in the NwAP to 1333.2 mg C m^{-2} in the CSS. On average, 34.2% of total microzooplankton biomass in the NwAP and NwR comprised HDF; they contributed over 60% to total biomass in the CSS. The proportional contribution of nanoHDF ranged between 11.3% and 85.1% of total HDF biomass, with highest contributions in the NwR. The contribution of microHDF to total HDF biomass was highest in the CSS. Depth-integrated HNF biomass ranged from 43.2 mg C m^{-2} in the NwR to 208.2 mg C m^{-2} in the CSS. The proportional contribution of these organisms to total microzooplankton biomass was 12.2%. Radiolarian contributed only small a fraction (average: 7.6%) to the total microzooplankton biomass.

Microzooplankton biomass was positively correlated with total Chl-*a* concentration (Fig. 7). Furthermore, HDF biomass was strongly related to the proportional contribution of the diatom fraction to total phytoplankton biomass (Fig. 7). Over the study period, HDF biomass was most strongly related to the proportion of diatoms in total phytoplankton biomass.

3.4. Microzooplankton grazing impact on major phytoplankton

Details of phytoplankton growth rates and microzooplankton grazing rates for all 21 dilution experiments are summarized in Tables 1 and 2. Data for some phytoplankton groups (e.g., diatoms, ANF, and ADF) at all depths in some stations and at SCM depths of stns 1, 3, and 13 were excluded from the analyses due to random apparent growth rates in the dilution series, high negative intrinsic growth rates or biomass concentrations of phytoplankton components that were too low before or after dilution incubations. Growth rates across all phytoplankton components ranged from 0.19 to 0.65 d^{-1}, averaging 0.31 ± 11 d^{-1}. Grazing rates ranged from 0.11 to 0.53 d^{-1}, averaging 0.23 ± 11 d^{-1}. Phytoplankton growth was not nutrient-limited in the experiments: average phytoplankton growth rates in nutrient addition treatments were indistinguishable from average phytoplankton growth rates without added nutrients, except in the case of diatoms (pairs test, $p < 0.05$, $n = 21$). The ratios of phytoplankton growth rates without added nutrients to those with added nutrients (μ/μ_n), were generally close to unity (Table 1 and Fig. 8). Grazing rate was significantly correlated with phytoplankton growth rate ($r = 0.83$, $p < 0.001$), but not with total Chl-*a* concentration or other

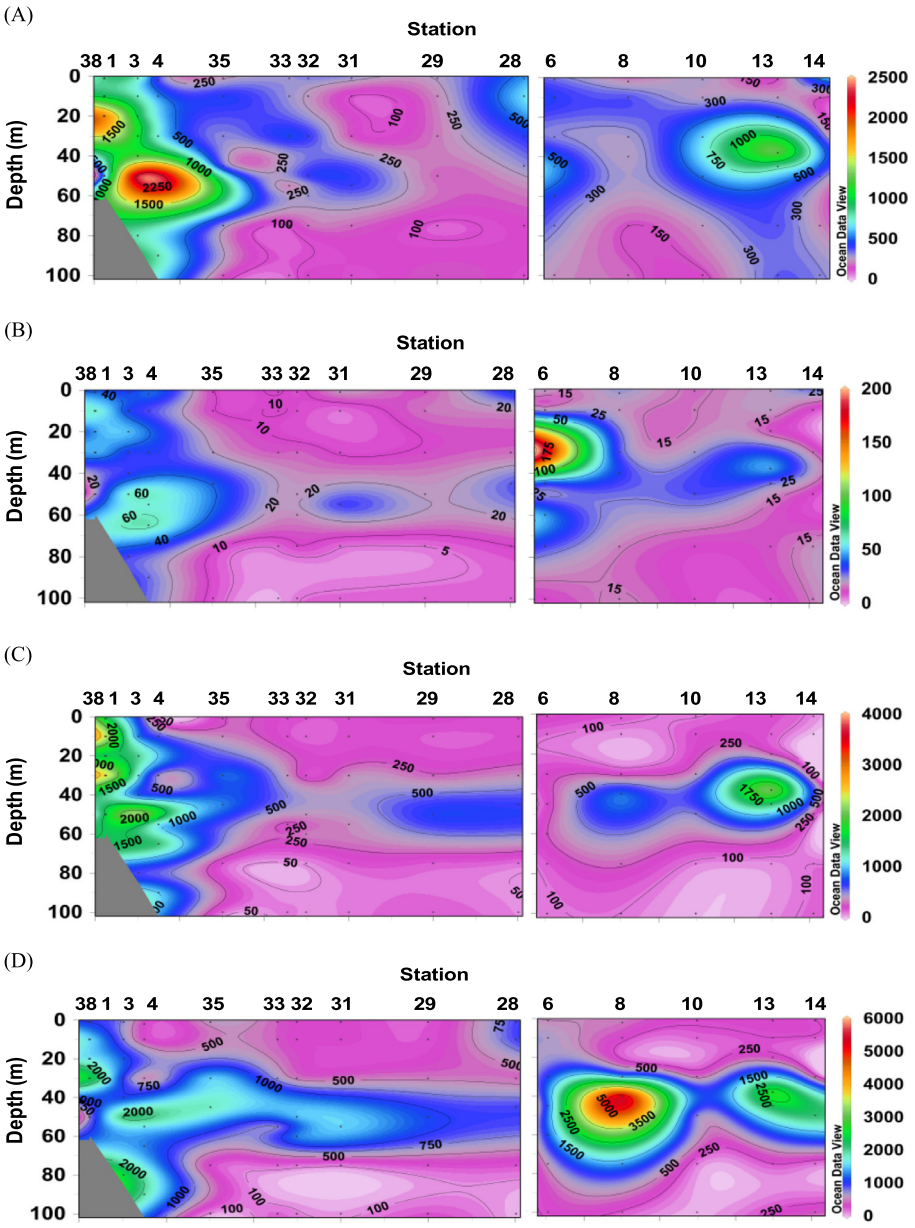

Fig. 5. Vertical section of microzooplankton composition in the western Arctic Ocean. (A) Heterotrophic nanoflagellate (HNF, cells ml^{-1}), (B) nano-heterotrophic dinoflagellate (nanoHDF, cells ml^{-1}), (C) micro-heterotrophic dinoflagellate (microHDF, cells l^{-1}), and (D) ciliates (cells l^{-1}).

environmental factors. There were no significant differences in phytoplankton growth and grazing rates among the three geographical regions. The daily proportion of Chl-*a* standing stock consumed by microzooplankton ranged from 11.3% to 42.1% (average, 19.2 ± 8.2%). Microzooplankton grazing consumed 44.1–92.6% of daily phytoplankton production. On average, more than half of daily phytoplankton production (72.7 ± 17.4%) was consumed by microzooplankton, but there was wide variation over the study period.

Growth rates of picophytoplankton, ANF and diatoms ranged from 0.14 to 0.68 d^{-1} (average, 0.39 ± 0.18 d^{-1}), from 0.17 to 0.59 d^{-1} (average, 0.33 ± 0.12 d^{-1}) and from 0.12 to 0.43 d^{-1} (average, 0.22 ± 0.08 d^{-1}), respectively (Table 2 and Fig. 8). Grazing rates on picophytoplankton, ANF and diatoms ranged from 0.15 to 0.62 d^{-1} (average, 0.32 ± 0.14 d^{-1}), from 0.15 to 0.46 (average, 0.26 ± 0.09 d^{-1}), and from 0.02 to 0.38 d^{-1} (average, 0.14 ± 0.08 d^{-1}), respectively. The growth rate of picophytoplankton and the grazing rate on these phytoplanktons exceeded rates for diatoms. The grazing rates on picophytoplankton exceeded phytoplankton growth rates at several stations in the CSS and NwR areas (Table 2). The percentage of primary production grazed by microzooplankton was 58.7–131.4% (average, 89.3 ± 20.5%) for picophytoplankton, 48.8–120.3% (average, 82.3 ± 22.5%) for ANF and 13.4–89.2% (average, 62.5 ± 20.5%) for diatoms. The grazing rates of microzooplankton on picophytoplankton exceeded those on diatoms. The microzooplankton grazing impact on diatoms was lowest among the phytoplankton groups, and therefore lowest in the CSS, where diatoms were the predominant primary producers.

4. Discussion

4.1. Hydrographic conditions and phytoplankton distribution

Warm water intrusion into the Pacific sector of the Arctic Ocean is an important driver that rapidly changes the horizontal and vertical fluxes of heat, salt and momentum (Shimada et al., 2005;

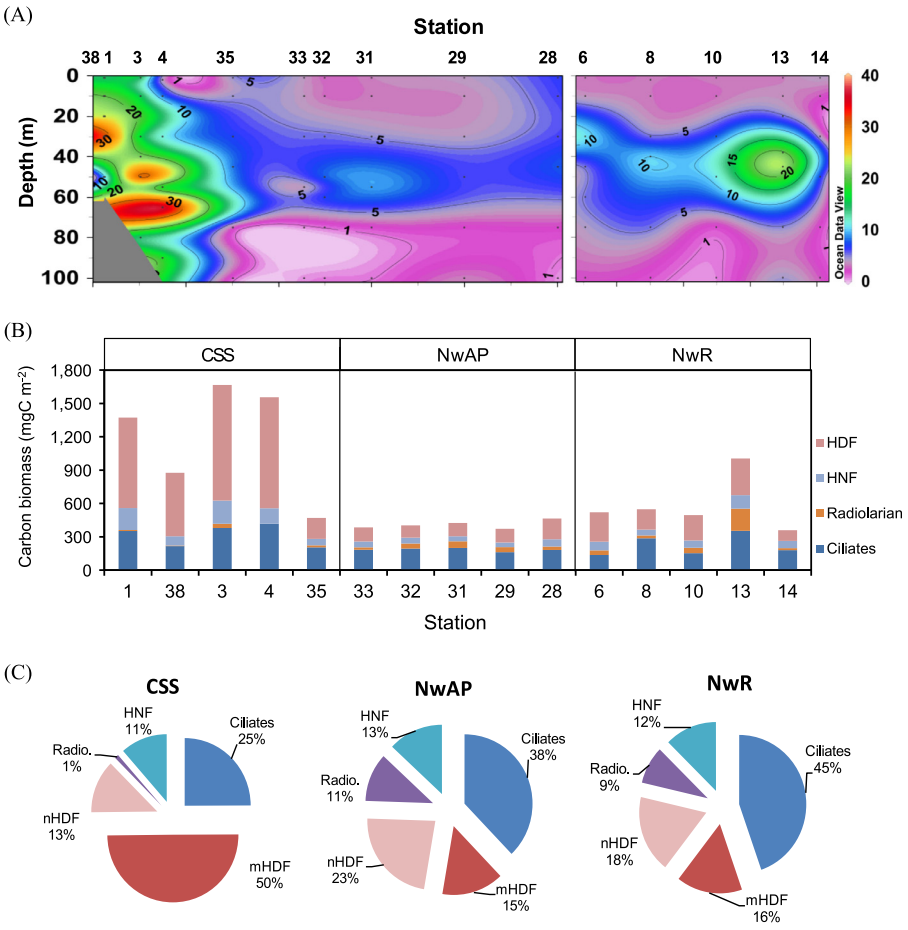

Fig. 6. Carbon biomass of microzooplankton in the western Arctic Ocean. (A) is vertical section, (B) is for cumulative carbon biomass from surface to 100 m, and (C) is for relative percent of microzooplankton community.

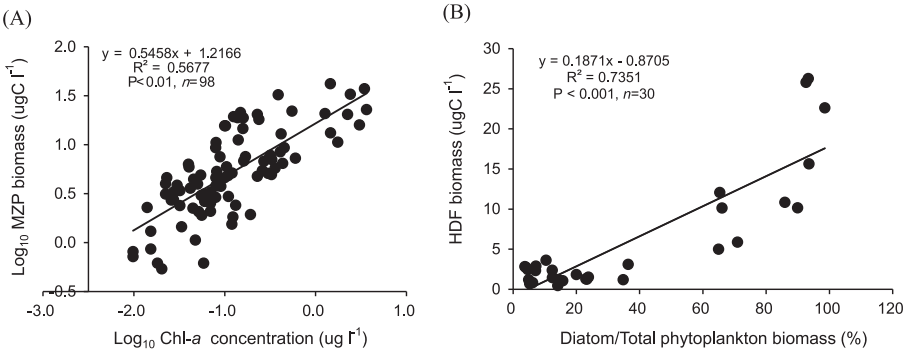

Fig. 7. Log–log relationship between microzooplankton (MZP) biomass and chlorophyll-a concentration (A), and heterotrophic dinoflagellate (HDF) biomass and fraction of diatom to total phytoplankton biomass (B) in the western Arctic Ocean.

Carmack and Melling, 2011). Changes in physical forcing and hydrographic conditions directly influence the plankton ecosystem across the western Arctic Ocean (Springer et al., 1987; Grebmeier and Harvey, 2005; Lane et al., 2008; Sukhanova et al., 2009). Our study area, in the western Arctic Ocean, included productive waters of the CSS, oligotrophic waters of the NwAP, and mesotrophic waters of the NwR (Fig. 2). Over the study period, we encountered diverse environmental conditions from heavy sea-ice cover (100%) to open water (< 10%), and a concomitant range of trophic conditions ranging from low Chl-*a* ($< 0.5\ \mu g\ l^{-1}$) in the NwAP to high diatom biomass (Chl-*a*: $3.6\ \mu g\ l^{-1}$) in the SCM layers of the CSS and the NwR (Table 1 and Fig. 3). Marked alterations in the composition and abundance of phytoplankton and microzooplankton were associated with changes in hydrographic and trophic conditions. In the CSS, high biomasses of phytoplankton and a predominance of diatoms were associated with advection of nutrient-rich Pacific water flowing northward from the Bering Sea into the Chukchi Sea (Codispoti et al., 2005). In the NwAP and in the surface layer of the NwR, the biomass of phytoplankton was low and dominated by picophytoplankton. The isolated pool of PSW was recognizable at depths shallower than 70 m in the northern part of NwAP. It formed a thick, warm layer between 40 and 70 m where the SCM was located. We also observed a warm-core eddy in the NwR (Fig. 2). This PSW-filled eddy transports nutrients and carbon from the CSS to the Canada Basin, where it may influence primary production and

Table 1
Summary parameters and results of grazing impact by microzooplankton at 10 m and SCM layer derived from dilution experiments. μ_n: phytoplankton growth rate, μ: phytoplankton growth rate without added nutrients, g: microzooplankton grazing rates, PS(%): daily phytoplankton standing stocks, PP(%): daily phytoplankton production grazed, r: correlation coefficient, $p < 0.05$, and ns: not significant. Values in brackets are standard error.

Station	Depth (m)	Initial Chl-*a* ($\mu g\ l^{-1}$)	μ (d^{-1})	μ_n (d^{-1})	g (d^{-1})	PS (%)	PP (%)	r^2	Temperature (°C)	Nitrate (μM)	Sea ice concentration (%)
1	10	0.15	0.43(0.11)	0.48(0.10)	0.33(0.14)	28.1	76.2	0.75	−1.48	0.30	90
3	10	0.10	0.28(0.05)	0.25(0.02)	0.13(0.07)	12.2	49.5	0.85	−1.42	0.20	95
4	10	0.09	0.35(0.09)	0.37(0.09)	0.25(0.14)	22.1	61.3	0.61	−1.42	0.43	85
	60	3.46	0.25(0.11)	0.25(0.10)	0.11(0.08)	10.4	47.1	0.79	−1.67	2.21	
6	10	0.03	0.30(0.04)	0.32(0.02)	0.27(0.04)	23.7	90.2	0.95	−1.22	0.29	56
	60	0.33	0.65(0.13)	0.52(0.13)	0.53(0.17)	41.1	86.1	0.76	−0.76	0.43	
10	10	0.03	0.45(0.05)	0.60(0.05)	0.29(0.06)	25.2	69.4	0.90	−1.09	0.29	60
	50	1.76	0.29(0.03)	0.28(0.02)	0.12(0.02)	11.3	44.1	0.93	−0.27	5.50	
13	10	0.04	0.19(0.03)	0.19(0.03)	0.14(0.05)	13.1	75.5	0.78	−1.10	0.29	74
14	10	0.03	0.24(0.04)	0.24(0.04)	0.18(0.06)	16.5	76.2	0.86	−0.94	0.64	30
	50	0.43	0.44(0.03)	0.42(0.03)	0.40(0.04)	31.6	92.6	0.96	−0.80	1.50	
28	10	0.04	0.36(0.02)	0.47(0.02)	0.30(0.04)	25.9	85.3	0.89	−1.34	0.43	75
	45	0.60	0.33(0.02)	0.34(0.02)	0.11(0.03)	10.4	36.4	0.89	−0.48	2.86	
29	10	0.03	0.22(0.04)	0.22(0.04)	0.20(0.05)	18.1	90.2	0.84	−1.26	0.86	68
	60	0.36	0.22(0.03)	0.15(0.03)	0.17(0.05)	15.6	79.2	0.84	−0.28	1.21	
31	10	0.06	0.20(0.05)	0.23(0.05)	0.18(0.06)	16.5	89.5	0.67	−1.21	0.21	31
	55	0.37	0.22(0.04)	0.14(0.04)	0.13(0.06)	12.2	61.8	0.62	−0.49	0.64	
35	10	0.09	0.34(0.04)	0.56(0.04)	0.31(0.05)	26.7	92.5	0.90	−1.38	0.16	0
	45	0.32	0.22(0.06)	0.13(0.06)	0.12(0.21)	11.3	57.3	0.61	−1.26	1.50	
38	10	0.44	0.27(0.04)	0.4(0.04)	0.21(0.05)	18.9	77.6	0.74	−1.15	0.43	0
	30	0.55	0.195(0.06)	0.18(0.06)	0.13(0.07)	12.2	68.7	ns	−1.59	6.29	

phytoplankton composition (Mathis et al., 2007; Nishino et al., 2011). In the Arctic Sea, previous studies indicated that there was enhanced phytoplankton biomass in the center of a warm-core eddy than that surrounding water (Rodríguez et al., 2003; Batten and Crawford, 2005). However, a study of the Sargasso Sea reported that the centers of warm-core eddies are nutrient-depleted zones with lower biological activity than surrounding areas because of the downwelling dynamics (e.g., Mouriño-Carballido, 2009). Therefore, biological responses to warm core eddies are much complicated and still unclear. In this study area, the warm-core eddy was clearly recognizable at stn 8. The low Chl-*a* concentration and a predominance of picophytoplankton at the center of the eddy were associated with low nutrient concentrations in the euphotic zone (Yun et al., 2015; La et al., 2015). Conversely, high Chl-*a* concentrations at SCM depths in stns 10 and 13 and a dominance of diatoms were consistent with small-scale phenomena, such as a continual supply of nutrients from depths underlying the euphotic zone of the eddy. Waters with high nitrate and silicate concentrations detected to a depth of 45 m are close to the upper boundary of the PWW (Yun et al., 2015; La et al., 2015). In summary, regional differences in phytoplankton assemblages across this study area were likely related to differences in hydrographic regimes.

4.2. Microzooplankton biomass and community structure

The microzooplankton biomass and composition measured during our study period were similar to those reported previously from waters of the high-latitude Arctic Ocean (Verity et al., 2002; Sherr et al., 2009). Microzooplankton biomass varied strongly among the stations, with the highest value in the CSS (average, $19.3 \pm 9.9\ \mu g\ C\ l^{-1}$) and lowest in the NwR (average, $3.96\ \mu g\ C\ l^{-1}$). Spatial distributions in measured parameters were associated with patterns of phytoplankton biomass and composition in the water masses. We corroborated a previous report that microzooplankton biomass in the Bering Sea (Sherr et al., 2009) increases with increasing phytoplankton biomass (Fig. 7), suggesting that microzooplankton populations have the capacity to increase rapidly in response to elevations in phytoplankton biomass; this rapid response of microzooplankton is probably attributable to high rates of population growth, which can match those of phytoplankton (Banse, 1992; Frost, 1993). HDF and ciliates were numerically the most important components of microzooplankton populations, but their densities differed among stations. Large athecate dinoflagellates; e.g., morphotypes similar to *Gyrodinium* and $>100\ \mu m$ in length, were especially abundant at stations where diatoms was dominant phytoplankton. The proportion of microHDF in total HDF biomass was highest in the CSS, where there was a dominance of diatoms. The contribution of nanoHDF to the total HDF biomass was highest in the NwR, where picophytoplankton was the dominant primary producer. The high proportion of HDF in the total microzooplankton biomass that we observed corroborates previous reports of a significant HDF biomass in Arctic waters, especially waters in which diatoms are dominant phytoplankton (Levinsen et al., 2000; Olson and Strom, 2002; Sherr et al., 2009, 2013). The coupling between HDF and diatom biomasses may express a top-down regulation relationship; i.e., the presence of an elevated biomass of HDF with powerful motility and large body size within diatom blooms may be indirectly attributable to increased abundance of diatoms, which serve as an alternate food source for mesozooplankton (Olson and Strom, 2002).

Ciliate populations were the dominant component of microzooplankton biomass (average, 48%) in the NwR (Fig. 6), and were particularly abundant at the center of the warm-core eddy (stn 8). Ciliates at this site seemed to be influenced by the relatively high temperature in the eddy. This suggestion is supported by previous reports that ciliate assemblages are strongly temperature-dependent (Montagnes and Weisse, 2000; Johansson et al., 2004; Aberle et al., 2007). Our limited observations (from a single transect through an eddy) make it difficult to assess the general significance of eddies in the regional microbial food webs. Although enhanced phytoplankton biomass in the center of a

Table 2
Summary of microzooplankton grazing impact on major phytoplankton derived from dilution experiments. μ_n: phytoplankton growth rate, μ: phytoplankton growth rate without added nutrients, g: microzooplankton grazing rates, PS(%): daily phytoplankton standing stocks, PP(%): daily phytoplankton production grazed, r^2: correlation coefficient, $p < 0.05$, ns: not significant. Values in brackets are standard error.

Station	Detph (m)	Phytoplankton compostion	μ (d^{-1})	μ_n (d^{-1})	g (d^{-1})	PS (%)	PP (%)	r^2
1	10	PicoP.	0.67(0.12)	0.48(0.12)	0.62(0.20)	46.2	93.7	0.55
		Diatom	0.23(0.07)	0.34(0.06)	0.13(0.08)	12.2	59.3	0.50
3	10	PicoP.	0.49(0.09)	0.46(0.08)	0.39(0.11)	32.3	83.5	0.53
		Diatom	0.15(0.05)	0.17(0.03)	0.09(0.11)	8.6	61.2	0.61
4	10	PicoP.	0.31(0.08)	0.31(0.07)	0.44(0.10)	35.6	131.5	0.90
		Diatom	0.34(0.13)	0.38(0.13)	0.25(0.09)	22.1	65.8	0.63
	60	PicoP.	0.43(0.09)	0.38(0.09)	0.23(0.11)	20.5	58.8	0.69
		Diatom	0.16(0.03)	0.32(0.03)	0.02(0.04)	2.0	13.4	0.51
6	10	PicoP.	0.68(0.11)	0.44(0.11)	0.61(0.15)	45.7	92.2	ns
		Diatom	0.20(0.11)	0.31(0.13)	0.17(0.16)	15.6	84.9	0.51
	60	PicoP.	0.18(0.04)	0.18(0.03)	0.20(0.04)	18.1	108.1	0.86
		ANF	0.19(0.12)	0.25(0.12)	0.26(0.20)	22.9	102.4	0.91
10	10	PicoP.	0.58(0.13)	1.06(0.13)	0.43(0.16)	34.9	79.2	0.76
		Diatom	0.24(0.10)	0.34(0.09)	0.12(0.09)	11.3	53.1	0.40
		ANF	0.46(0.04)	0.83(0.03)	0.33(0.04)	28.1	75.1	0.91
		ADF	0.32(0.08)	0.30(0.08)	0.16(0.12)	14.8	54.0	0.68
	50	PicoP.	0.36(0.10)	0.40(0.10)	0.26(0.12)	22.9	58.5	0.68
		Diatom	0.26(0.01)	0.26(0.01)	0.08(0.01)	7.7	33.5	ns
		ADF	0.38(0.04)	0.32(0.04)	0.25(0.05)	22.1	70.0	0.56
13	10	PicoP.	0.15(0.06)	0.16(0.02)	0.19(0.03)	17.3	126.4	0.91
		Diatom	0.19(0.04)	0.17(0.03)	0.12(0.05)	11.3	65.1	0.62
14	10	PicoP.	0.17(0.03)	0.20(0.03)	0.15(0.05)	13.9	89.9	0.78
		Diatom	0.28(0.06)	0.31(0.06)	0.18(0.09)	16.5	67.3	0.67
		ANF	0.60(0.12)	0.48(0.13)	0.46(0.17)	36.9	81.9	0.69
	50	PicoP.	0.17(0.04)	0.27(0.02)	0.19(0.03)	17.3	110.0	0.94
		ANF	0.32(0.07)	0.24(0.07)	0.40(0.10)	33.0	120.4	0.79
28	10	PicoP.	0.58(0.06)	0.72(0.06)	0.39(0.08)	32.3	73.0	0.87
		Diatom	0.44(0.07)	0.45(0.06)	0.38(0.08)	31.6	89.8	0.84
	45	PicoP.	0.45(0.16)	0.82(0.16)	0.51(0.22)	40.0	110.8	0.65
		Diatom	0.33(0.07)	0.40(0.05)	0.08(0.07)	7.7	27.4	0.49
		ANF	0.34(0.12)	0.35(0.09)	0.15(0.12)	13.9	48.8	0.56
29	10	PicoP.	0.33(0.09)	0.42(0.09)	0.32(0.12)	27.4	96.9	0.70
		ANF	0.17(0.03)	0.25(0.03)	0.20(0.04)	18.1	115.5	0.93
	60	PicoP.	0.24(0.04)	0.17(0.03)	0.20(0.04)	18.1	85.0	0.90
		Diatom	0.12(0.05)	0.16(0.02)	0.09(0.03)	8.6	77.4	0.86
		ANF	0.32(0.05)	0.23(0.04)	0.17(0.04)	15.6	57.1	0.74
31	10	PicoP.	0.49(0.05)	0.25(0.02)	0.29(0.03)	25.2	65.3	ns
		Diatom	0.12(0.06)	0.17(0.03)	0.07(0.04)	6.8	58.9	ns
		ANF	0.43(0.04)	0.61(0.04)	0.29(0.06)	25.2	72.2	0.92
	55	PicoP.	0.24(0.05)	0.16(0.05)	0.21(0.06)	18.9	89.2	0.79
		ANF	0.18(0.05)	0.24(0.04)	0.14(0.06)	13.1	80.4	0.64
35	10	PicoP.	0.73(0.16)	0.58(0.16)	0.46(0.21)	36.9	71.0	0.58
		Diatom	0.21(0.07)	0.39(0.05)	0.16(0.07)	14.8	78.1	0.73
		ANF	0.29(0.07)	0.30(0.07)	0.36(0.10)	30.2	120.1	0.71
	45	PicoP.	0.27(0.06)	0.20(0.04)	0.17(0.05)	15.6	78.5	0.68
		Diatom	0.14(0.05)	0.11(0.05)	0.09(0.07)	8.6	67.9	ns
		ANF	0.32(0.05)	0.29(0.04)	0.28(0.04)	24.4	88.6	0.64
38	10	PicoP.	0.27(0.08)	0.37(0.08)	0.29(0.11)	26.7	105.6	0.51
		Diatom	0.17(0.03)	0.33(0.02)	0.12(0.02)	11.3	72.3	0.81
	30	PicoP.	0.42(0.16)	0.39(0.16)	0.27(0.22)	23.7	69.0	ns
		Diatom	0.15(0.07)	0.16(0.04)	0.09(0.06)	8.6	62.1	0.49
		ANF	0.45(0.03)	0.34(0.03)	0.23(0.04)	20.5	56.8	ns

warm-core eddy has been reported previously (Rodríguez et al., 2003; Batten and Crawford, 2005), to our knowledge, unusually high ciliate abundances at the centers of warm-core eddies have not. Hence, the microbial food web in the warm-core eddy we studied likely has a more important functional role in pelagic ecosystems than previously recognized. Ciliate biomass was highest in the CSS and at stn 13, but the ciliate proportion in total microzooplankton biomass was highest in the NwAP. Although, ciliates biomass was significantly correlated with Chl-*a* concentration ($r=0.69$, $p<0.001$, $n=92$), ciliate proportional contribution to microzooplankton biomass was significantly correlated with picophytoplankton ($r=0.52$, $p<0.005$, $n=30$) and ANF biomass ($r=0.39$, $p<0.05$, $n=30$). Since large naked ciliates (>150 μm in length) were also observed in the CSS and in the SCM layer at stn 13, where diatoms were predominant in the phytoplankton, we cannot completely rule out the possibility that large ciliates may be important grazers of chain forming-diatoms in high Arctic waters, which is the case in the Bering Sea (Sherr et al., 2013). Thus, a tight coupling between microzooplankton population size and phytoplankton composition likely indicates that food supply is among the most important factors controlling the spatial dynamics of microzooplankton assemblage composition. Reports

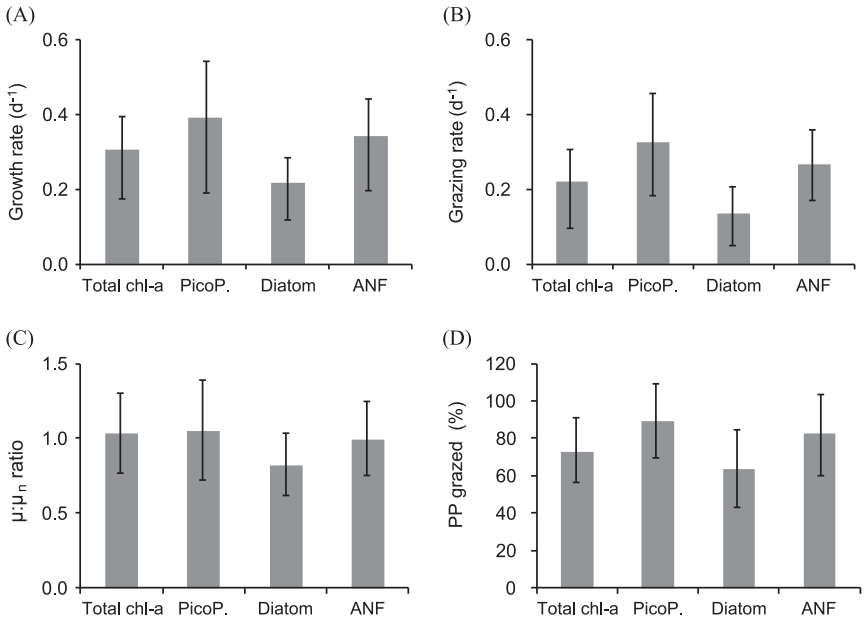

Fig. 8. The growth rate (A), grazing rate (B), μ:μ_n ratio (C) and microzooplankton grazing impacts (%PP) (D) on major phytoplankton groups. PicoP, picophytoplankton; ANF, autotrophic nanoflagellate; μ_n, phytoplankton growth rate estimated from treatments with added nutrients; and μ, phytoplankton growth rate estimated from treatments with no nutrients added. The error bars represent the standard deviation.

on combined studies of ciliate, HDF and HNF biomasses in Arctic waters are rare (Hansen et al., 1996; Ratkova and Wassmann, 2002; Verity et al., 2002). HNF have been reported as dominant in microzooplankton biomass when the productivity of the water mass is low, e.g., under the land-fast ice in winter–spring (Vaqué et al., 2008) or during summer (off Svalbard; Seuthe et al., 2011). We found that HNF were very small (2–6 μm) and constituted a minor portion of the microzooplankton assemblage, accounting for 9–18% of microzooplankton biomass in our study area. Since HNF are potentially important grazers of bacteria and picophytoplankton (Sherr and Sherr, 1987; Becquevort et al., 2000; Calbet et al., 2001; Guillou et al., 2001; Shinada et al., 2003), we would expect them to have a significant role as grazers of picophytoplankton in this study area.

4.3. *Impacts of microzooplankton grazing on major phytoplankton groups*

We used dilution experiments to estimate phytoplankton growth and microzooplankton grazing rates. Both specific growth rates and grazing rates estimated from the dilution experiments were in good agreement with reported summer values for Arctic waters (Liu et al., 2002; Olson and Strom, 2002; Verity et al., 2002; Strom and Fredrickson, 2008), though higher than those reported for parts of the high-latitude Arctic Ocean (Sherr et al., 2009; Calbet et al., 2011). Among phytoplankton groups, growth rate was highest in the picophytoplankton (average, 0.39 ± 0.18 d^{-1}) and lowest in the diatoms (average, 0.22 ± 0.08 d^{-1}). In general, small phytoplankton cells grow faster than large cells; the small surface area to volume ratios give small phytoplankton advantages in competition for dissolved nutrients (Eppley et al., 1970). This view is supported by the allometric theory of phytoplankton metabolic and growth rates (Raven and Kubler, 2002). The ratio μ/μ_n, which is an index of nutrient limitation, indicates an absence of apparent nutrient limitation when values approach unity. In our experiments, the ratio had an average value of 1.0 for total Chl-*a*, 1.0 for picophytoplankton and ANF, and 0.8 for diatom (Fig. 8). We did not detect large differences in phytoplankton growth rates between treatments with and without nutrient enrichment (except in the case of diatoms). The lack of a nutrient effect may be attributable to the short incubation times. For this reason, overall regulation of the pelagic system seems to fit a top-down control better than a bottom-up control, at least during our period of study, although low nutrient concentrations may have effects on phytoplankton assemblage composition and overall biomass.

The grazing impacts of microzooplankton on phytoplankton were substantial, accounting for an average of 71.7 ± 17.2% (range: 44.1–92.6%) of daily phytoplankton production. Although some studies have reported low microzooplankton grazing rates in parts of the high Arctic Ocean (Sherr et al., 2009; Calbet et al., 2011), our estimates are close to the range of 64–97% (average, 77%) reported for the early summer in the Barents Sea (Verity et al., 2002). Recent reports for some parts of the Chukchi and Beaufort Seas describe much lower microzooplankton grazing rates on phytoplankton (average, 36%) during summer. Sherr et al. (2009) attributed these low microzooplankton grazing rates to senescence of the diatom bloom. When a phytoplankton bloom is senescent, grazers, even when abundant, may strongly reduce their grazing rate (Calbet et al., 2011). We did not observe senescent diatoms during our study. In a previous analysis of western Arctic plankton, the average Chl-*a* concentration was 10-fold higher than the level we measured. It is likely that variability in the trophic status affects microzooplankton grazing rates.

Microzooplankton gazing impacts were higher in the NwR and NwAP than in the CSS, even though growth and grazing rates were not significantly different among regions (Table 1). In the NwR and NwAP, the phytoplankton was dominated by appropriately sized prey (e.g., picophytoplankton and ANF) except in the SCM layer at stns 10 and 13, where diatoms were dominant. When phytoplankton cells are within an appropriate section of the particle size spectrum, microzooplankton grazing is intense and promotes nutrient regeneration that supports further divisions of algal cells. In the CSS, which was dominated by chain-forming diatoms, microzooplankton consumed an average of 63.4 ± 13.1% of the phytoplankton production, and an average of 36.6% of photosynthetic carbon was transferred to larger grazers. These estimates

do not take account of the sinking of phytoplankton cells out of suspension. The results and conclusions of the experiments are supported by our estimates of microzooplankton grazing impact on major phytoplankton groups. We did not observe microzooplankton preferences for the dominant components of the phytoplankton; instead, these consumers preferentially grazed on picophytoplankton and ANF, rather than on diatoms. Rates of microzooplankton grazing on picophytoplankton and ANF in the CSS were lower than rates in the NwR and NwAP. At some stations, microzooplankton grazed over 100% of production by picophytoplankton and ANF, regardless of the biomass and dominance of these algal groups. This observation is congruent with previous reports that microzooplankton graze preferentially on smaller phytoplankton with high growth rates (Strom and Welschmeyer, 1991). The marked impact of grazing, especially on picophytoplankton (average proportion of production consumer: $89.3 \pm 20.5\%$, maximum: 131.4%), demonstrates that during early summer season microzooplankton grazing may control the growth of small phytoplankton and at times reduce overall phytoplankton biomass. In general, there is an indication of balanced food dynamics between picophytoplankton production and microzooplankton grazing. Diatoms were a relatively poor food source for microzooplankton in comparison with picophytoplankton and ANF. The grazing impact on diatoms was lower in the CSS (average, $47.4 \pm 28.6\%$) than in other regions (average, $63.7 \pm 19.5\%$). The large size of diatom cells probably accounts for their unsuitability as food items for microzooplankton. Nevertheless, microzooplankton grazed $>50\%$ of diatom production when large HDF were abundant in the microzooplankton. In previous studies large HDF have been observed grazing on chain-forming diatoms (Strom and Fredrickson, 2008; Suffrian et al., 2008; Sherr et al., 2009; Sherr et al., 2013). Large HDF, such as *Gymnodinium* sp., and *Protoperidinium* sp., are able to engulf prey items larger than themselves (Strom et al., 2001; Jeong et al., 2004; Sherr and Sherr, 2007). High grazing rates on diatoms in the NwR and CSS might also be attributable to ciliates; large naked ciliates, which may be dominant elements in the microzooplankton of the Bering Sea, have been observed feeding on diatoms in northern Norwegian waters (Sherr et al., 2013) (Fig. 6). Thus, microzooplankton are important mediators of mortality of both large and small phytoplankton cells.

5. Conclusions

We confirmed the important role played by microzooplankton in the functioning of pelagic ecosystems at high-latitudes in the Arctic Ocean. During early summer, the microzooplankton assemblage was a significant component controlling phytoplankton biomass and composition. Furthermore, these consumers may play a pivotal role in the transfer of organic carbon to higher trophic levels. We also suggest that there is little export of carbon fixed by phytoplankton out of upper water layers because microbial food web recycling of organic carbon is a dominant process in the upper water of the study area.

Climate change may affect protist dynamics directly (e.g., through changing temperature, nutrient, pCO_2) or indirectly (e.g., through changing food sources and predators) and these shifts may be amplified in polar regions (Caron and Hutchins, 2013). The western Arctic Ocean is undergoing rapid warming, and plankton assemblage may be adjusting their distributions to reflect changes in their environment (Steele et al., 2008; Zhang et al., 2010). A recent modeling study reported that a warming climate may alter the balance between phytoplankton growth and microzooplankton grazing in the ocean (Chen et al., 2012). Therefore, the results of our study may be used to provide a baseline for assessments of how future environmental changes will affect the microbial food web structure at high-latitudes in the Arctic Ocean

Acknowledgments

The authors thank the captain and crew of the *IBRV* ARAON who were most helpful in all shipboard operations. This research was a part of the Project titled 'K-PORT (KOPRI, PM13020)', funded by the MOF, Korea. Also, this research was supported by Inha University Research Grant (INHA-49278).

Reference

Aagaard, K., Coachman, L.K., Carmack, E.C., 1981. On the halocline of the Arctic Ocean. Deep-Sea Res. I 28, 529–545.
Aberle, N., Lengfellner, K., Sommer, U., 2007. Spring bloom succession, grazing impact and herbivore selectivity of ciliate communities in response to winter warming. Ocenologia 150, 668–681.
Ashjian, C.J., Campbell, R.G., Welch, H.E., Butler, M., Van Keuren, D., 2003. Annual cycle in abundance, distribution, and size in relation to hydrography of important copepod species in the western Arctic Ocean. Deep-Sea Res. I 50, 1235–1261.
Banse, K., 1992. Grazing, temporal changes of phytoplankton concentrations, and the microbial loop in the open sea. In: Falkowski, P.G., Woodhead, A.D. (Eds.), Primary Productivity and Biogeochemical Cycles in the Sea. Plenum, New York, pp. 409–440.
Batten, S.D., Crawford, W.R., 2005. The influence of coastal origin eddies on oceanic plankton distributions in the eastern Gulf of Alaska. Deep-Sea Res. II 52, 991–1009.
Becquevort, S., Menon, P., Lancelot, C., 2000. Differences of the protozoan biomass and grazing during spring and summer in the Indian sector of the Southern Ocean. Polar Biol. 23, 309–310.
Burkill, P.H., Mantoura, R.F.C., Llewellyn, C.A., Owens, N.J.P., 1987. Microzooplankton grazing and selectivity of phytoplankton in coastal waters. Mar. Biol. 93, 581–590.
Bøsheim, K.Y., Bratbak, G., 1987. Cell volume to cell carbon conversion factors for a bacterivorus *Monas* sp. enriched from sea waters. Mar. Ecol. Prog. Ser. 36, 171–175.
Calbet, A., 2008. The trophic roles of microzooplankton in marine systems. ICES J. Mar. Sci. 65, 325–331.
Calbet, A., Landry, M.R., 2004. Phytoplankton growth, microzooplankton grazing, and carbon cycling in marine systems. Limnol. Oceanogr. 40, 51–57.
Calbet, A., Saiz, E., 2005. The ciliate–copepod link in marine ecosystems. Aquat. Microb. Ecol. 38, 157–167.
Calbet, A., Landry, M.R., Nunnery, S., 2001. Bacteria–flagellate interactions in the microbial food web of the oligotrophic subtropical North Pacific. Aquat. Microb. Ecol. 23, 283–292.
Calbet, A., Saiz, E., Almeda, R., Movilla, J.I., Alcaraz, M., 2011. Low microzooplankton grazing rates in the Arctic Ocean during a *Phaeocystis pouchetii* bloom (Summer 2007): factor artifact of the dilution technique? J. Plankton Res. 33, 687–701.
Campbell, R.G., Sherr, E.B., Ashjian, C.J., Plourde, S., Sherr, B.F., Hill, V., Stockwell., D. A., 2009. Mesozooplankton prey preference and grazing impact in the western Arctic Ocean. Deep-Sea Res. II 56, 1274–1289.
Carmack, E., Melling, H., 2011. Warmth from the deep. Nat. Geosci. 4, 7–8.
Carmack, E., Wassmann, P., 2006. Food webs and physical-biological coupling on pan-Arctic shelves: unifying concepts and comprehensive perspectives. Prog. Oceanogr. 71, 446–477.
Caron, D.A., Hutchins, D.A., 2013. The effects of changing climate on microzooplankton grazing and community structure: drivers, predictions and knowledge gaps. J. Plankton Res. 35, 235–252.
Chen, B., Landry, M.R., Huang, B., et al., 2012. Dose warming enhance the effect of microzooplankton grazing on marine phytoplankton in the Ocean? Limnol. Oceanogr. 57, 519–526.
Codispoti, L.A., Flagg, C., Kelly, V., Swift, J.H., 2005. Hydrographic conditions during the 2002 SBI process experiments. Deep-Sea Res. II 52, 3199–3226.
Comiso, J.C., Parkinson, C.L., Gersten, R., Stock, L., 2008. Accelerated decline in the Arctic sea ice cover. Geophys. Res. Lett. 35, L01703, http://dx.doi.org/10.1029/2007GL031972.
Edler, L., 1979. Phytoplankton and chlorophyll recommendations for biological studies in the Baltic Sea. Balt. Mar. Biol. Pub. 5, 13–25.
Eppley, R.W., Reid, F.M.H., Stickland, J.D.H., 1970. Estimates of phytoplankton crop size, growth rate and primary production. Bull. Scripps Inst. Oceanogr. Univ. Calif. 17, 33–42.
Frost, B.W., 1993. A modelling study of processes regulating plankton standing stock and production in the open subArctic Pacific Ocean. Prog. Oceanogr. 32, 17–56.
Grebmeier, J.M., Harvey, H.R., 2005. The western Arctic shelf-basin interactions (SBI) project: an overview. Deep Sea Res. II 52, 3109–3115.
Guillou, L., Jacquet, S., Chrétiennot-Denet, M., Vaulot, D., 2001. Grazing impact of two small heterotrophic flagellates on *Prochlorococcus* and *Synechococcus*. Aquat. Microb. Ecol. 26, 201–207.
Hansen, B., Bjørnsen, P.K., Hansen, P.J., 1994. The size ratio between planktonic predators and their prey. Limnol. Oceanogr. 39, 395–403.

Hansen, B.W., Christiansen, S., Pedersen, G., 1996. Plankton dynamics in the marginal ice zone of the central Barents Sea during spring: carbon flow and structure of the grazer food chain. Polar Biol. 16, 115–128.
Holland, M.M., Bitz, C.M., Hunke, E.C., Lipscomb, W.H., Schramm, J.L., 2006. Influence of the sea ice thickness distribution on polar climate in CCSM3. J. Clim. 19, 2398–2414.
Irigoien, X., Flynn, K.J., Harris, R.P., 2005. Phytoplankton blooms: a 'loophole' in microzooplankton grazing impact? J. Plankton Res. 27, 313–321.
Jeong, H.J., Yoo, Y.D., Kim, S.T., Kang, N.S., 2004. Feeding by the heterotrophic dinoflagellate *Protoperidinium bipes* on the diatom *Skeletonema costatum*. Aquat. Microb. Ecol. 36, 171–179.
Johansson, M., Gorokhova, E., Larsson, U., 2004. Annual variability in ciliate community structure, potential prey and predators in the open northern Baltic Sea proper. J. Plankton Res. 26, 67–80.
La, H.S., Kang, M.H., Dahms, H.-U., Ha, H.K., Yang, E.J., Kim, Y.N., Chung, K.H., 2015. Characteristics of the sound-scattering layer in the Pacific summer water, Arctic Ocean. Deep-Sea Res. II 120, 114–123, http://dx.doi.org/10.1016/j.dsr2.2015.01.005.
Landry, M.R., Hassett, R.P., 1982. Estimating the grazing impact of marine micro-zooplankton. Mar. Biol. 67, 283–288.
Lane, P.V.Z., Llinas, L., Smith, S.L., Pilz, D., 2008. Zooplankton distribution in the western Arctic during summer 2002: hydrographic habitats and implications for food chain dynamics. J. Mar. Syst. 70, 97–133.
Levinsen, H., Nielsen, T.G., 2002. The trophic role of marine pelagic ciliates and heterotrophic dinoflagellates in Arctic and temperate coastal ecosystems: a cross-latitude comparison. Limnol. Oceanogr. 47, 427–439.
Levinsen, H., Nielsen, T.G., Hansen, B.W., 1999. Plankton community structure and carbon cycling on the western coast of Greenland during the stratified summer situation. II. Heterotrophic dinoflagellates and ciliates. Aquat. Microb. Ecol. 16, 217–232.
Levinsen, H., Turner, J.T., Nielsen, T.G., Hansen, B.W., 2000. On the trophic coupling between protists and copepods in Arctic marine system. Mar. Ecol. Prog. Ser. 204, 65–77.
Liu, H., Suzuki, K., Saino, T., 2002. Phytoplankton growth and microzooplankton grazing in the subArctic Pacific Ocean and the Bering Sea during summer 1999. Deep-Sea Res. I 49, 363–375.
Mathis, J.T., Pickart, R.S., Hansell, D.A., Kadko, D., Bates, N.R., 2007. Eddy transport of organic carbon and nutrients from the Chukchi Shelf: Impact on the upper halocline of the western Arctic Ocean. J. Geophys. Res. 112, C05011, http://dx.doi.org/10.1029/2006JC003899.
Menden-Deuer, S., Lessard, E., 2000. Carbon to volume relationships for dinoflagellates, diatoms, and other protist plankton. Limnol. Oceanogr. 45, 569–579.
Michaels, A.F., Caron, D.A., Swanberg, N.R, Howse, F.A., Michaels, C.M., 1995. Planktonic sarcodines (Acantharia, Radiolaria, Foraminifera) in surface waters near Bermuda: abundance, biomass and vertical flux. J. Plankton Res. 17, 131–163.
Montagnes, D.J.S., Weisse, T., 2000. Fluctuating temperatures affect growth and production rates of planktonic ciliates. Aquat. Microb. Ecol. 21, 97–102.
Mouriño-Carballido, B., 2009. Eddy-driven pulses of respiration in the Sargasso Sea. Deep-Sea Res. I 56, 1242–1250.
Nielsen, T.G., Hansen, N., 1995. Plankton community structure and carbon cycling in the western coast of Greenland during and after the sedimentation of a diatom bloom. Mar. Ecol. Prog. Ser. 125, 239–257.
Nishino, S., Itoh, M., Kawaguchi, Y., Kikuchi, T., Aoyama, M., 2011. Impact of an unusually large warm-core eddy on distributions of nutrients and phytoplankton in the southwestern Canada Basin during late summer/early fall 2010. Geophys. Res. Lett. 38, L16602, http://dx.doi.org/10.1029/2011GL047885.
Olson, M.B., Strom, S.L., 2002. Phytoplankton growth, microzooplankton herbivory and community structure in the southeast Bering Sea: insight into the formation and temporal persistence of an *Emiliania huxleyi* bloom. Deep-Sea Res. II 49, 5969–5990.
Parson, T.R., Maita, Y., Lalli, C.M., 1984. A Manual of Chemical and Biological Methods for Seawater Analysis. Pergamon Press, Oxford p. 173.
Putt, M., Stoecker, D.K., 1989. An experimentally determined carbon–volume ratio for marine oligotrichous ciliates from estuarine and coastal waters. Limnol. Oceanogr. 34, 1097–1103.
Ratkova, T.N., Wassmann, P., 2002. Seasonal variation and spatial distribution of phyto-and protozooplankton in the central Barents Sea. J. Mar. Syst. 38, 47–75.
Raven, J.A., Kubler, J.E., 2002. New light on the scaling of metabolic rate with the size of algae. J. Phycol. 38, 11–16.
Reckermann, M., Veldhuis, M.J., 1997. Trophic interactions between picophytoplankton and micro- and nanozooplankton in the western Arabian Sea during the NE monsoon 1993. Aquat. Microb. Ecol. 12, 263–273.
Rodríguez, F., Varela, M., Fernández, E., Zapata, M., 2003. Phytoplankton and pigment distributions in an anticyclonic slope water oceanic eddy (SWODDY) in the southern Bay of Biscay. Mar. Biol. 143, 995–1011.
Saiz, E., Calbet, A., 2011. Copepod feeding in the ocean: scaling patterns, composition of their diet and the bias of estimates due to microzooplankton grazing during incubation. Hydrobiologia 666, 181–196.
Sakshaug, E., Slagstad, D., 1992. Sea ice and wind: effects on primary productivity in the Barents Sea. Atmos. Ocean 30, 579–591.
Seuthe, L., Iversen, K.R., Narcy, F., 2011. Microbial processes in a high-latitude fjord (Kongsfjorden, Svalbard): II. Ciliates and dinoflagellates. Polar Biol. 34, 751–766.
Sherr, E.B., Sherr, B.F., 1987. High rates of consumption of bacteria by pelagic ciliates. Nature 325, 710–711.
Sherr, E.B., Sherr, B.F., 2002. Significance of predation by protists in aquatic microbial food webs. Antonie van Leeuwenhoek 81, 293–308.
Sherr, E.B., Sherr, B.F., 2007. Heterotrophic dinoflagellates: a significant component of microzooplankton biomass and major grazers of diatoms in the sea. Mar. Ecol. Prog. Ser. 352, 187–197.
Sherr, E.B., Sherr, B.F., Fessenden, L., 1997. Heterotrophic protists in the central Arctic Ocean. Deep-Sea Res. II 48, 1665–1682.
Sherr, E.B., Sherr, B.F., Wheeler, P.A., Thompson, K., 2003. Temporal and spatial variation in stocks of autotrophic and heterotrophic microbes in the upper water column of the central Arctic Ocean. Deep-Sea Res. I 50, 557–571.
Sherr, E.B., Sherr, B.F., Hartz, A.J., 2009. Microzooplankton grazing impact in the Western Arctic Ocean. Deep-Sea Res. II 56, 1264–1273.
Sherr, E.B., Sherr, B.F., Ross, C., 2013. Microzooplankton grazing impact in the Bering Sea during spring sea ice conditions. Deep-Sea Res. II 94, 57–67.
Shimada, K., Itoh, M., Nishino, S., McLaughlin, F., Carmack, E., 2005. Halocline structure in the Canada Basin of the Arctic Ocean. Geophys. Res. Lett. 32, L03605.
Shinada, A., Ban, S., Ikeda, T., 2003. Seasonal changes in nano/micro-zooplankton herbivory and heterotrohpic nanoflagellates bacterivory off Cape Esan, Southwestern Hokkaido, Japan. J. Ocenaogr. 59, 609–618.
Springer, A., Murphy, E., Roseneau, D., McRoy, C.P., Cooper, B., 1987. The paradox of pelagic food webs in the northern Bering Sea-I. Seabird food habits. Cont. Shelf Res. 7, 895–911.
Steele, M., Ermold, W., Zhang, J., 2008. Arctic Ocean surface warming trends over the past 100 years. Geophys. Res. Lett. 35, L02614, http://dx.doi.org/10.1029/2007GL031651.
Strom, S.L., Fredrickson, K.A., 2008. Intense stratification leads to phytoplankton nutrient limitation and reduced microzooplankton grazing in the southeastern Bering Sea. Deep-Sea Res. II 55, 1761–1774.
Strom, S.L., Welschmeyer, N.A., 1991. Pigment specific rates of phytoplankton growth and microzooplankton grazing in the open sub-Arctic Pacific Ocean. Limnol. Oceanogr. 36, 50–63.
Strom, S.L., Brainard, M.A., Holmes, J.L., Olson, M.B., 2001. Phytoplankton blooms are strongly impacted by microzooplankton grazing in coastal North Pacific waters. Mar. Biol. 138, 355–368.
Suffrian, K., Simonelli, P., Nejstgaard, J.C., Putzeys, S., Carotenuto, Y., Antia, A.N., 2008. Microzooplankton grazing and phytoplankton growth in marine mesocosms with increased CO_2 levels. Biogeosciences 5, 1145–1156.
Sukhanova, I.N., Flint, M.V., Pautova, L.A., Stockwell, D.A., Grebmeier, J.M., Sergeeva, V.M., 2009. Phytoplankton of the western Arctic in the spring and summer of 2002: structure and seasonal changes. Deep-Sea Res. II 56, 1223–1236.
Taylor, A.G., Landry, M.R., Selph, K.E., Yang, E.J., 2011. Biomass, size structure and depth distributions of the microbial community in the eastern equatorial Pacific. Deep-Sea Res. II 58, 342–357.
Vaqué, D., Guadayol, Ó., Peters, F., Felipe, J., Angel-Ripoll, L., Terrado, R., Lovejoy, C., Pedrós-Alió, C., 2008. Seasonal changes in planktonic bacterivory rates under the ice-covered coastal Arctic Ocean. Limnol. Oceanogr. 53, 2427–2438.
Verity, P.G., Langdon, C., 1984. Relationships between lorica volume, carbon, nitrogen and ATP content of tintinnids in Narragansett Bay. J. Plankton Res. 6, 859–868.
Verity, P.G., Stocker, D.K., Sieracki, M.E., Nelson, J.R., 1993. Grazing, growth and mortality of microzooplankton during the 1989 North Atlantic spring bloom at 47°N, 18°W. Deep-Sea Res. II 40, 1793–1814.
Verity, P.G., Wassmann, P., Frischer, M.E., Howard-Jones, M.H., Allen, A.E., 2002. Grazing of phytoplankton by microzooplankton in the Barents Sea during early summer. J. Mar. Syst. 38, 109–123.
Walsh, J.J., Dieterle, D.A., Maslowski, W., Whitledge, T.E., 2004. Decadal shifts in biophysical forcing of Arctic marine food webs: numerical consequences. J. Geophys. Res. 109, C05031, http://dx.doi.org/10.1029/ 2003JC001945.
Yang, E.J., Hyun, J.J., Kim, D., Park, J., Kang, S.H., Shin, H.C., Lee, S.H., 2012. Mesoscale distribution of protozooplankton communities and their herbivory in the western Scotia Sea of the Southern Ocean during the austral spring. J. Exp. Mar. Biol. Ecol. 428, 5–15.
Yun, M.S., Kim, B.K., Joo, H.T., Yang, E.J., Nishino, S., Chung, K.H., Kang, S.H., Lee, S.H., 2015. Regional productivity of phytoplakton in the western Arctic Ocean during early summer in 2010. Deep-Sea Research II 120, 61–71, http://dx.doi.org/10.1016/j.dsr2.2014.11.023.
Zhang, J., Spitz, Y.H., Steele, M., Ashjian, C, Campbell, R., Berline, R., Matrai, P., 2010. Modeling the impact of declining sea ice on the Arctic marine planktonic ecosystem. J. Geophys. Res. 115, C10015, http://dx.doi.org/10.1029/2009JC005387.